CHEMISTRY & CHEMICAL TECHNOLOGY

Chem. Chem. Technol., 2023,
Vol. 17, No. 3, pp. 636–645

Chemical Technology

REMOVAL OF PHENOL FROM WATER USING AN ACTIVATED CARBON PREPARED FROM *JUNIPERUS THURIFERA* TREE

***Khiouani Adel*[1, ✉], *Hachani Salah Eddine*[2], *Meklid Abdelhek*[2]**

https://doi.org/10.23939/chcht17.03.636

Abstract. The present paper aims to study the feasibility of using an activated carbon prepared by *Juniperus thurifera* tree as an adsorbent to remove phenol from water by adsorption. The impact of initial phenol concentration, contact time, pH, and adsorbent mass on phenol adsorption capacity was investigated. It was reported that the highest adsorption capacity is achieved at pH=3.4, phenol concentration of 50 mg/L, adsorbent mass of 100 mg, and time 24 h. Freundlich, Langmuir, and Temkin isotherm equations were used to best fit our experimental data. Hence, Freundlich model was found to be the best model with $R^2 = 0.9893$. The thermodynamic results revealed that the adsorption of phenol onto the activated carbon was spontaneous and exothermic. Furthermore, the adsorption kinetic study indicated that the adsorption process follows the pseudo-first-order kinetic model.

Keywords: activated carbon, *Juniperus thurifera* tree, phenol, adsorption.

1. Introduction

Like air, water is an essential element of life. Without water, no organism whether a plant or animal can live. Safe drinking water is the water that can be delivered to the user and is safe for drinking, food preparation, personal hygiene, and washing. The water must meet the required the chemical, physical and biological quality standards at the point of supply to the users.[1]

The huge progression in urbanization and industrialization expose safe water to pollution.[2] Phenol is considered one of the most common dangerous pollutants to human health and the environment. This water contaminant is issued from effluents discharging of various industries including plastic, paper, pulp, paint, petrochemical, wood products, and pharmaceuticals. Phenol can affect most of the body organs such as brain, eyes, liver, kidneys, and lungs. In even cases, it can cause genetic damage.[3-4] This health risk increases at higher phenol concentrations. The world health organization has set the maximum concentration of phenol in drinking water to be 1 μg/L,[5] whereas the environmental protection agency (EPA) has set the maximum concentration of phenol in wastPhenol removal from both drinking water and wastewater has received considerable attention from academia and industry. Many experimental approaches such as biodegradation, chemical oxidation, catalytic oxidation, membrane separation, and adsorption have been used to remove phenol from aqueous media.[7-11] The adsorption technique is a simple, effective, and low-cost method for water treatment. This process uses clay,[12-14] carbon nanotubes,[15,16] and activated carbon as adsorbents to eliminate the required water contaminant.[17-21]

Juniperus thurifera is a tree belongs of *Cupressaceae* family with very variable leaf scales. It is an exclusively western Mediterranean species, present in France, Spain, Italy, Morocco, and Algeria. In Algeria, this tree is only present in the Aurès with individuals scattered in the cedar groves or in the form of monospecific stands of a few tens of hectares. *Juniperus thurifera* is of ecological, floristic, socio-economic, and cultural interest.[22]

In the present scientific contribution, we attempt to use a new activated carbon obtained from *Juniperus thurifera* tree as an effective adsorbent for phenol removal from water. The influences of phenol initial concentration, elemental phenol concentration, contact time, pH, and mass of adsorbent on phenol adsorption onto the activated carbon have been investigated. Kinetic isotherms at the equilibrium were conducted to well fit the experimental data. Thermodynamic parameters have been calculated for deep understanding of the adsorption process.

[1] Laboratory Chemistry of Materials and Living Organisms Activity and Reactivity (LCMVAR), Faculty of Material Sciences, Department of Chemistry, University of Batna 1, Algeria
[2] Laboratory of Applied Chemistry (LCA), University of Biskra, BP 145, 07000 Biskra, Algeria
✉ *khiouaniadel@gmail.com*

2. Experimental

2.1. Reagents

The properties of the used reagents were collected in Table 1.

2.2. Sample Preparation

Our activated carbon was prepared from *Juniperus thurifera* tree. The plant material was well washed for with distilled water for several times and then dried after that it was chemically treated with nitric acid at a concentration of 10 % for 24 hours. The obtained precursor was washed again with distilled water, dried at 373 K for 24 hours and then carbonized at temperature of 723 K for two hours in Nabertherm laboratory oven. The resulting carbonized matter was washed with distilled water and then dried at 373 K for 24 hours.

2.3. Sample Characterization

The obtained activated carbon has been analyzed by X-rays diffraction analysis using Bruker D8 Advanced diffractometer operating at 40 kV. Scans were recorded within 2θ varying from 10 to 80°. FTIR analysis has been carried out using Shimadzu spectrophotometer. Small weight of each prepared activated carbon was mixed with KBr powder and pressed to get transparent sample. Spectra were obtained within wavenumber ranging from 400 to 4000 cm^{-1}. The studied activated carbon has been the subject of scanning electron microscopy SEM analysis to study the morphology. This analysis was conducted using TESCAN VEGA3 laboratory equipment operating at 20 kV under high vacuum. The sample was coated with gold prior to analysis.

Experiments of batch mode adsorption were conducted using UV/Visible spectrophotometer to investigate the effects of phenol initial concentration, contact time, pH and adsorbent dose on phenol adsorption capacity onto the activated carbon. The experimental data of the current study was tested using Langmuir, Freundlich and Temkin isotherms. The phenol adsorption capacity (q_e) was calculated using the following equation:[23]

$$q_e = \frac{(C_0 - C_e)V}{m} \quad (1)$$

where C_0 is the initial concentration of phenol in the solution (mg/L), C_e is the equilibrium concentration of phenol (mg/L), V is the volume of the solution (L), and m is the mass of the adsorbent (mg).

Table 1. Properties of the used reagents

Nomenclature	Phenol	Nitric acid
Chemical formula	C_6H_6O	HNO_3
Appearance	White crystalline solid	Transparent liquid
Purity assay (%)	99.0	Pure
Cas	108-95-2	7697-37-2
Molecular weight (g/mol)	94.11	63.01
Volumetric mass (kg/L)	1.06	1.38
Company	AnalaR NORMAPUP	Cheminova

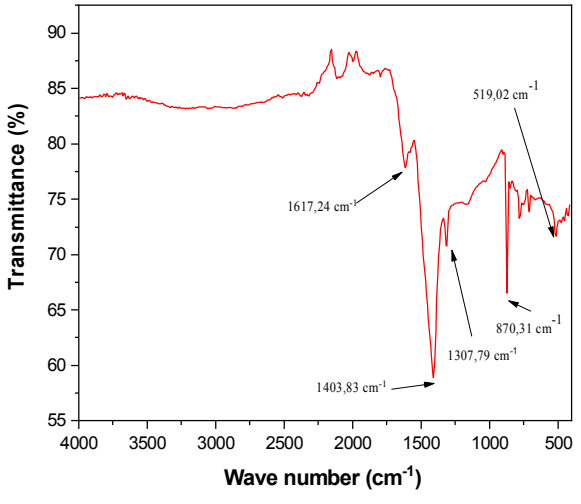

Fig. 1. FTIR spectrum of the prepared activated carbon at 723 K

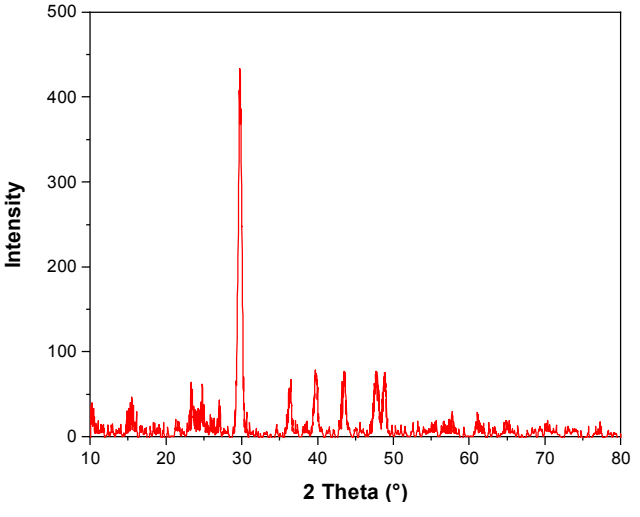

Fig. 2. XRD pattern of the studied activated carbon

3. Results and Discussion

3.1. Characterization of the Prepared Activated Carbon

The properties of carbon have been studied using the following techniques:

3.1.1. Fourier Transform Infrared Spectroscopy (FTIR) Analysis

The obtained activated carbon has been the subject of FTIR analysis to investigate surface functional groups of the prepared activated carbon. Measurements were recorded in the range of wavenumber varies from 500 to 4000 cm^{-1}.

As can be seen from Fig. 1, FTIR spectrum corresponding to our activated carbon has mainly a band located at 1617 cm^{-1}, this last one is attributed to the presence of C=O bond stretching vibration. C=C vibration bond can be detected with the presence of an intense peak located at 1403 cm^{-1}.[24] However, peaks observed at 1307, 870 and 519 cm^{-1}, respectively. These bands are dedicated to the presence of =C–H and C–H, respectively in the tested sample.[25]

3.1.2. X-Ray Diffraction (XRD) Results

The activated carbon under probe has been tested using X-ray diffraction (XRD) analysis to investigate its structural properties. The XRD pattern of the studied sample is shown in Fig. 2. It can be seen that the obtained spectrum exhibits a crystalline structure with a principal peak located at $2\theta = 29.86°$. Similar results have been reported in the literature.[23]

3.1.3. Scanning Electron Microscopy SEM Results

The morphology of the activated carbon has an important effect on the absorption of the contaminant; a highly porous structure is required for maximal adsorption efficiency. Scanning electron microscopy SEM is used as a powerful tool to study the microstructure of the activated carbon under investigation. SEM images of the activated carbon with different magnifications as shown in Fig. 3 revealed that the activated carbon samples have external surfaces containing porous structures with different shapes and sizes. The formation of such microstructure maybe is a result of the volatile compounds released during the activation stage.

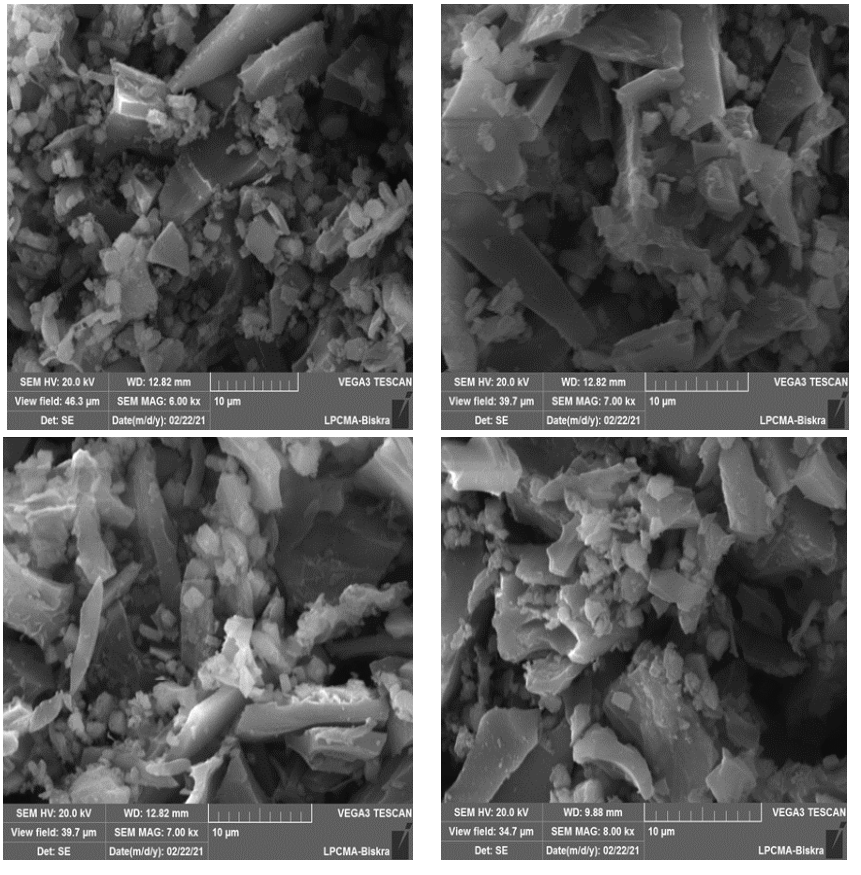

Fig. 3. SEM images of the prepared activated carbon sample with different magnifications

3.2. The Influence of Adsorbent Mass

Phenol adsorption on the activated carbon was studied by modifying the adsorbent mass from (100, 150, 200, 250, 300, and 350 mg). The experiments conditions were kept at pH = 3.4, temperature of 293 K and initial phenol concentration C_0 = 50 mg/L under agitation of 400 r/min for 24 hours. The sorption capacity is strongly influenced by the surface area and the diameter of the grains of the concerned porous material. High surface area of the sorbent, the diameter of its pores and the chemical nature of its surface are required for maximum sorption capacity. Fig. 4 exhibits the adsorption capacity variations as a function of adsorbent mass. It can be seen that the adsorption capacity decreases with the increase of adsorbent mass. This decrease in the adsorption intensity may be due to a large amount of adsorbent, which effectively reduces the unsaturated sites of the adsorption and the surface area.[26]

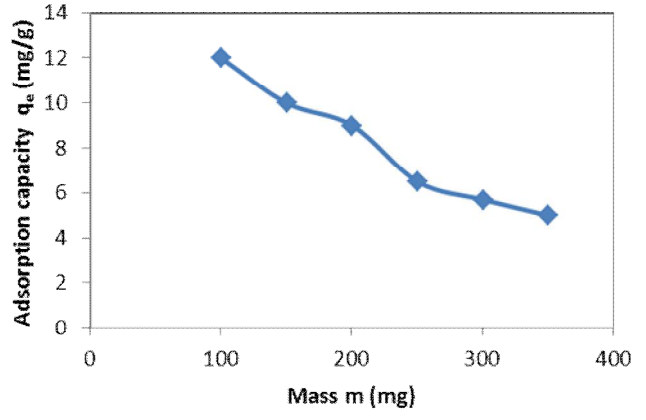

Fig. 4. Adsorption capacity variations as a function of adsorbent mass

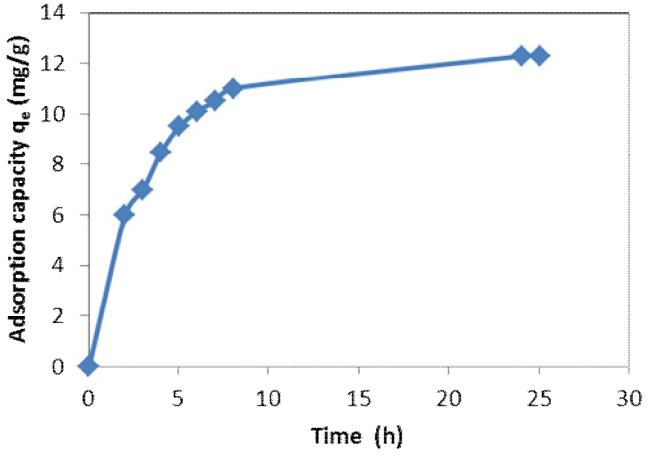

Fig. 5. Adsorption capacity variations as a function of contact time

3.3. The Effect of Contact Time

The impact of different contact times of the adsorbent on phenol removal capacity is experimentally investigated according to following experiment conditions V = 50 mL, m = 100 mg, agitation= 400 r/min, T = 294.5 K and initial phenol concentration C_0= 50 mg/L. The variations of phenol removal capacity as a function of contact time are shown in Fig. 5. It is evident that the removal proportion increases with the increase of contact time between the activated carbon and phenol. The amount of the adsorbed phenol increased with contact time after the first 2 hours then the adsorption process reached the equilibrium after 24 hours with q_e = 12.3 mg/g.

3.4. Effect of pH

The pH of a solution has a significant impact on the adsorption process. This is attributed to the amount of surface charge of the adsorbent, amount of ionization of the material present in the solution as well as separation of the functional groups present in the active adsorbing sites distributed in the adsorbent. In the current study, the effect of pH on phenol adsorption on the examined activated carbon samples was studied with pH ranging from 3.45 to 11.15 according to experiment conditions (V = 50 m, C_0 = 50 mg/L, T = 293.5 K, m = 100 mg, agitation = 400 r/min, and time = 24 h). Fig. 6 exhibits the variations of the adsorption capacity as a function of pH. It is evident that with the increase of pH value from 3.45 to 11.15, the phenol adsorption capacity decreases from 14 to 3.5 mg/g. At lower pH (<7), the decrease in phenol absorption capacity with rising pH may be due to the competition between hydrogen ions and phenol for the adsorption sites. At higher pH values (>7), phenol is in the form of a salt which loses its negative charge easily and becomes difficult to adsorb. Besides, the presence of OH^- ions inhibits phenol ions from being adsorbed on activated carbon.[27]

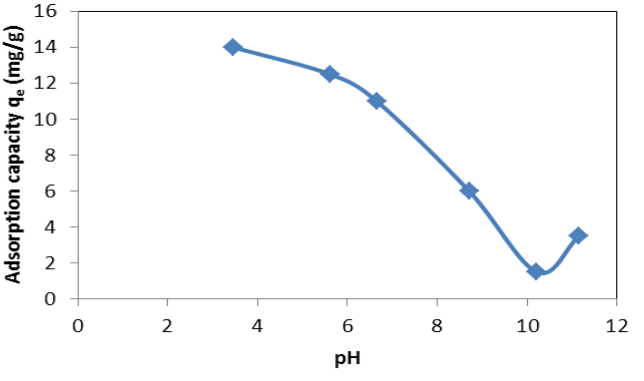

Fig. 6. The changes of the adsorption capacity as a function of pH

3.5. The Effect of Initial Phenol Concentration

The adsorption capacity of activated carbon was studied as a function of initial phenol concentration variations. The adsorption experiments were performed in conditions (V = 50 mL, T =294 K, m = 100 mg, agitation = 400 r/min, and time = 24 h) with different initial concentrations of phenol (5, 10, 20, 30, 40, and 50 mg/L).

As can be seen from Fig. 7 and Table 2, the amount of the absorbed phenol was increased from 2 to 11.5 mg/g with the increase of the phenol concentration from 5 to 50 mg/L indicating that the elemental phenol concentration plays an important role in the absorption of phenol on the activated carbon. The phenol present in solution at higher concentrations cannot interact with the active adsorption sites of the activated carbon samples due to their saturation.[28]

Table 2. Results of the impact of initial phenol concentration on the adsorption capacity

C_0(phenol) (mg/L)	5	10	20	30	40	50
C_e(phenol) (mg/L)	1	3	7	14	21	27
q_e (mg/g)	2	3.5	6.5	8	9.5	11.5
C_e/q_e (g/L)	0.5	0.86	1.08	1.75	2.21	2.35
LnC_e	0	1.10	1.95	2.64	3.04	3.30
Lnq_e	0.69	1.25	1.87	2.08	2.25	2.44

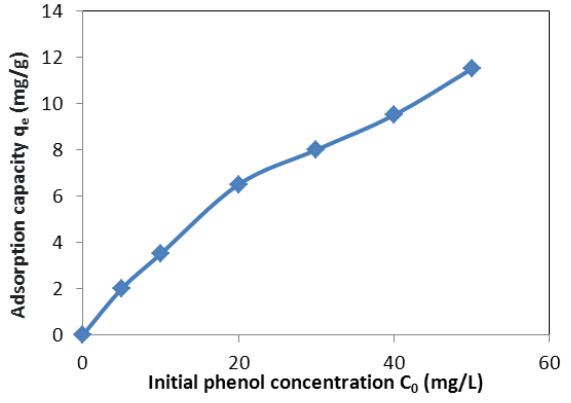

Fig. 7. The variations of the adsorption capacity q_e as a function of initial phenol concentration C_0

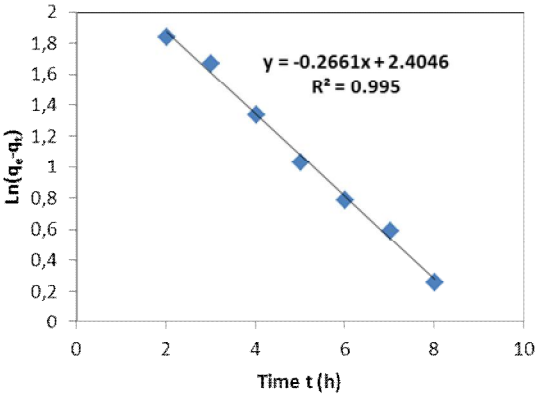

Fig. 8. Ln($q_e - q_t$) variations as a function of time

3.6. Adsorption Kinetics

The kinetic studies provided important information about the phenol adsorption mechanism. Three adsorption models are proposed to fit the experimental data reported in the current study.

3.6.1. The Pseudo-First-Order Kinetic Adsorption

This model has been proposed by Lagergren to evaluate the adsorption of solid/liquid systems, it can be expressed in linear and integral form using the following equation:[29]

$$Ln(q_e - q_t) = -k_1 t - \ln(q_e) \qquad (2)$$

where k_1 is the adsorption constant rate given in h^{-1}, q_e is the phenol adsorption capacity at equilibrium (mg/g), and q_t is the phenol adsorption capacity (mg/g) at time t (h). In this case, the plot of Ln($q_e - q_t$) *versus* t should provide a straight line within k_1 and q_e projected from the slope and intersection of the straight line can be determined, respectively (Fig. 8). The results of pseudo-first-order kinetic adsorption and its parameters are given in Tables 3 and 4.

Table 3. Results of pseudo-first-order kinetic adsorption

t (h)	2	3	4	5	6	7	8
C_e (mg/g)	38	36	33	31	29.8	29	28
q_t	6	7	8.5	9.5	10.1	10.5	11
$q_e - q_t$	6.3	5.3	3.8	2.8	2.2	1.8	1.3
Ln($q_e - q_t$)	1.84	1.67	1.34	1.03	0.79	0.59	0.26

Table 4. Experimental adsorption capacity and the pseudo-first-order constants

$q_{e\,(exp)}$ (mg/g)	$q_{e\,(Pseudo\text{-}first\text{-}order)}$ (mg/g)	k_1 (h^{-1})	R^2
12.3	11.0739	0.2661	0.9950

Table 5. Results of pseudo-second-order kinetic adsorption

t (h)	2	3	4	5	6	7	8
C_e (mg/g)	38	36	33	31	29.8	29	28
q_t (mg/g)	6	7	8.5	9.5	10.1	10.5	11
t/q_t (h g/mg)	0.33	0.43	0.47	0.53	0.59	0.67	0.73

3.6.2. The pseudo-second-order kinetic adsorption

This type of kinetic adsorption is described using the following formula:[30]

$$\frac{t}{q_t} = \frac{1}{k_2 q_e^2} + \frac{t}{q_e} \quad (3)$$

where k_2 is the adsorption constant rate of the pseudo-second-order and its unit (g/mg h). The plot of t/q_t as a function of t should give a straight line; q_e and k_2 can be calculated from slope and intercept of the curve, respectively (Fig. 9). The results corresponding to pseudo-second-order kinetic adsorption and its parameters are collected in Tables 5 and 6.

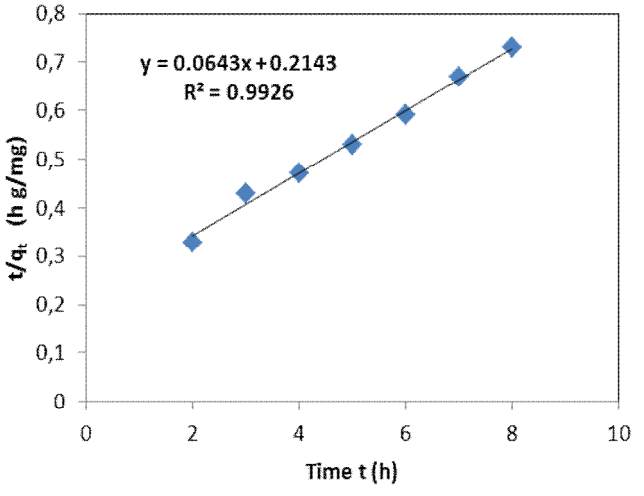

Fig. 9. $\frac{t}{q_t}$ variations as a function of time

Table 6. Experimental adsorption capacity and the obtained pseudo-second-order parameters

$q_{e\,(exp)}$ (mg/g)	$q_{e\,(Pseudo\text{-}second\text{-}order)}$ (mg/g)	k_1 (g/(mg h))	R^2
12.3	15.5520	0.0193	0.9926

3.6.3. The Intraparticle Diffusion

The intraparticle diffusion model is presented in the following equation:[31]

$$q_t = k_{int} t^{0.5} + C \quad (4)$$

In equation (4), k_{int} is the adsorption constant rate of the intraparticle diffusion model (mg/g $h^{-0.5}$). The plot giving the variations of q_t as a function of $t^{0.5}$ should be a straight line. k_{int} and C can be calculated from slope and intercept of the curve, respectively (Fig. 10). The results of intraparticle diffusion model and its parameters are resumed in Tables 7 and 8.

Table 7. Results of intraparticle diffusion model

t (h)	2	3	4	5	6	7	8
C_e (mg/L)	38	36	33	31	29.8	29	28
$t^{0.5}$ ($h^{0.5}$)	1.41	1.73	2	2.24	2.45	2.65	2.83
q_t (mg/g)	6	7	8.5	9.5	10.1	10.5	11

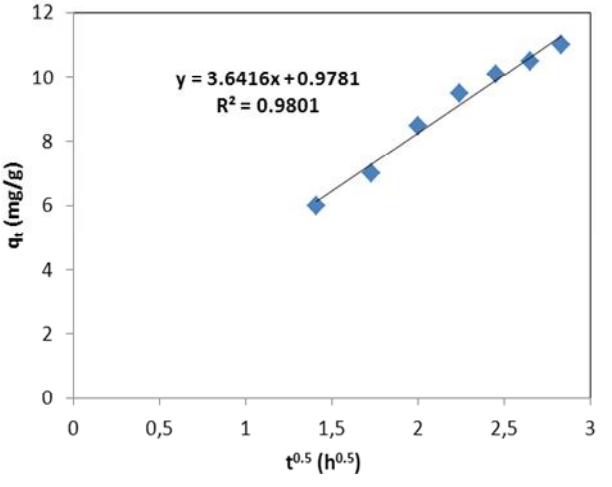

Fig. 10. The variations of q_t as a function of $t^{0.5}$

Table 8. Experimental adsorption capacity and the obtained intraparticle diffusion parameters

$q_{e\,(exp)}$ (mg/g)	k_{int} (mg/g h)	C (mg/g)	R^2
12.3	3.6416	0.9781	0.9801

The pseudo-first-order, the pseudo-second-order and the intra-particle diffusion model have been used to assess the kinetics of the phenol and the activated carbon interactions. The adsorption constant rate k, the adsorption capacity q_e, and the correlation coefficient R^2 were calculated for the three tests showing that the values of the correlation coefficient of the pseudo-first-order kinetic model was highest $R^2 = 0.9950$ indicating the model's applicability to describe the adsorption process with an experimental $q_e = 12.3$ mg/g, this result is close to the computed one obtained from the pseudo-first-order model $q_e = 11.07$ mg/g suggesting that the pseudo-first-order model fits the experimental data better than the other kinetic models.

3.7. Isotherm Kinetics

The experimental data of the current study was tested using Langmuir, Freundlich, and Temkin isotherms. These isotherm models are describing as following:

3.7.1. Langmuir Isotherm

This model is based on the following points:

– The presence of specific sites for adsorption on the adsorption surface.

– Each site can only adsorb one molecule.

– The surface is covered to the maximum extent with one layer.

– The adsorption energy is constant.

– Activity in a particular site does not affect activity in neighboring sites, so there are no interactions between adsorbed molecules.

Langmuir model is expressed as:[32]

$$\frac{C_e}{q_e} = \frac{1}{q_{\max} K_L} + \frac{C_e}{q_{\max}} \qquad (5)$$

K_L is Langmuir adsorption constant (L/mg), q_{max} is the Langmuir constant related to the maximum monolayer adsorption capacity (mg/g).[33] The graph giving the changes of $\frac{C_e}{q_e}$ as a function of C_e is a line with a slope $\frac{1}{q_{\max}}$ and an ordinate at the origin $(\frac{1}{q_{\max} K_L})$, this allows the determination of the two Langmuir parameters as given in Table 9. In this study, the curve monitoring Langmuir model is as follows:

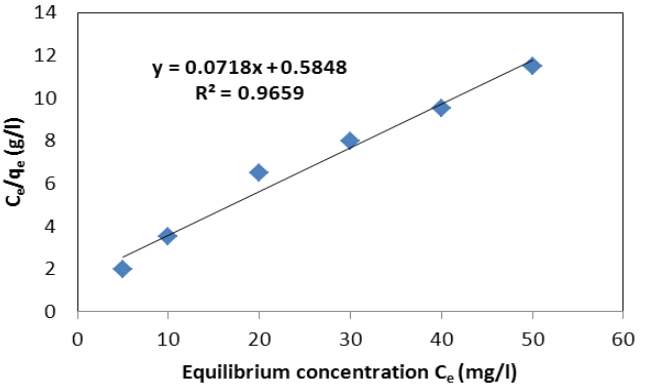

Fig. 11. The changes of $\frac{C_e}{q_e}$ as a function of C_e

Table 9. Langmuir isotherm constants

K_L (L/mg)	q_{max} (mg/g)	R^2
0.1228	13.9276	0.9659

3.7.2. Freundlich Isotherm

A Freundlich isotherm is a mathematical expression describing the adsorption equilibrium between a fluid (adsorbate) and a solid material (adsorbent). The Freundlich equation is an empirical expression representing the isothermal variations of adsorption of a liquid or gas on a solid material surface, rationalized by Freundlich as an empirical relation that can be expressed as:[34]

$$Lnq_e = LnK_F + \frac{LnC_e}{n} \qquad (6)$$

K_F (mg/g) and $\frac{1}{n}$ are two constants dedicated to the capacity of adsorption and the intensity of adsorption, respectively. The curve exhibiting Lnq_e as a function of LnC_e is a line with a slope $\frac{1}{n}$ and an ordinate at the origin LnK_F. This allows the determination of the two Freundlich parameters as given in Table 10. In our case of study, the curve representing Freundlich model is as follows:

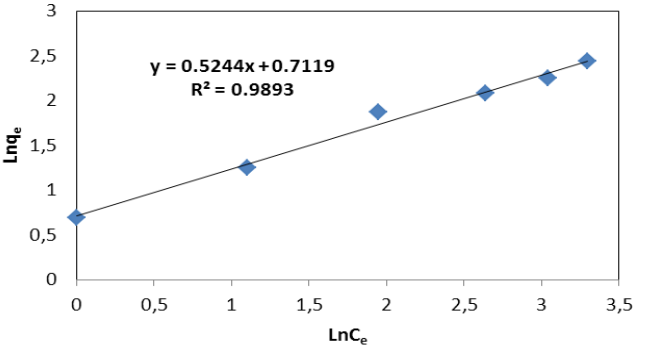

Fig. 12. The variations of Lnq_e as a function of LnC_e

Table 10. Freundlich isotherm constants

K_F (mg/g)	n_F	R^2
2.0379	1.9070	0.9893

3.7.3. Temkin Isotherm

It consists of the assumption that the heat of absorption decreases linearly with the increase of solid surface recovery rate.[35] Temkin equation formulated for the adsorption of gases to solids and transposed to the liquid phase. The form of Temkin's isotherm at equilibrium is written as follows:[36]

$$q_e = BLnK_T + BLnC_e \quad (7)$$

where $B = \frac{RT}{b}$, $b = \Delta G$; Temkin's energy constant (J/mol) and K_T represents the factor that explicitly takes into account the interactions between the components of the adsorption system. The graphical representation of q_e as a function of LnC_e is a line with a slope B and an ordinate at the origin BLnK_T, which permits calculating Temkin model parameters as mentioned in Table 11. In the current research, the curve describing the Temkin model is as follows:

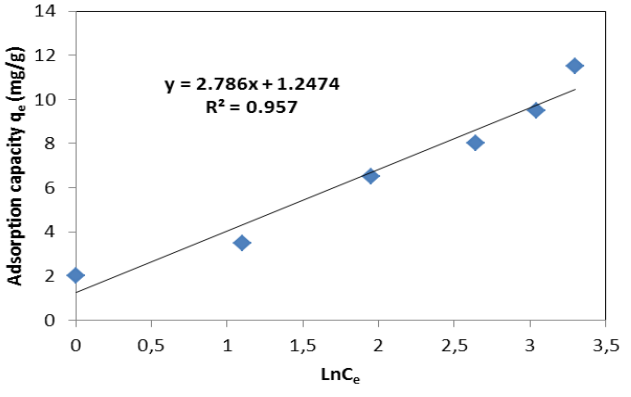

Fig. 13. The changes of q_e as a function of LnC_e

Table 11. Temkin isotherm constants

K_T	B = $(RT)/\Delta G$	R^2
9.3320	B = 2.7860, ΔG = 0.8773 kJ/mol	0.9570

3.7.4. Equilibrium Modeling Analysis

The comparison of correlation coefficient R^2 values corresponding to the proposed isotherm models demonstrated that Freundlich having $R^2 = 0.9893$ (the highest R^2 among the three models) is the best model to describe the isothermal adsorption of phenol on the activated carbon.

3.8. Thermodynamic Parameters

Thermodynamic parameters such as the free energy changes ΔG, the enthalpy ΔH, the entropy ΔS, and the diffusion coefficient K_d associated to the phenol adsorption onto the activated have calculated using the following formulas:[27]

$$K_d = \frac{q_e}{C_e} \quad (8)$$

$$\Delta G = -RTLnK_d \quad (9)$$

ΔG also can obtained using this mathematical relation:

$$\Delta G = \Delta H - T\Delta S \quad (10)$$

$$-RTLnK_d = \Delta H - T\Delta S \quad (11)$$

$$LnK_d = \frac{\Delta S}{R} - \frac{\Delta H}{TR} \quad 12)$$

The adsorption capacity q_e was calculated at different temperatures (298, 303, 313, and 323 K) considering the following experimental conditions: $C_{0\,(phenol)}$ = 50 mg/L; V = 50 mL; m = 100 mg; agitation = 400 r/min, and R = 8.314 J/mol K.

The variations of LnK_d as a function of $\frac{1}{T}$ give a line with slope $\frac{\Delta H}{R}$ and an ordinate at the origin $\frac{\Delta S}{R}$, this allows the determination of the two function ΔH and ΔS.

Table 12 and Fig. 14 present the obtained results.

ΔS = - 1.9704 J/(mol K), ΔH = - 2.2899 kJ/mol

The negative values of ΔG in the temperature range of 298-323 K indicate that the adsorption process was spontaneous. In addition, the negative value of ΔS indicates a decrease in randomness at the solid/liquid interface during phenol adsorption on the activated carbon. The change in free energy values in enthalpy ΔH and Gibbs free energy ΔG for physical adsorption in general.

Table 12. Thermodynamic results of the studied adsorption

T (°C)	25	30	40	50
T (K)	298	303	313	323
$1/T$ (K^{-1})	0.0033557	0.0033003	0.0031948	0.0030959
C_e (mg/L)	25	24.6	24.4	24
q_e (mg/g)	12.5	12.7	12.8	13
$K_d = C_e/q_e$	2	1.94	1.91	1.85
LnK_d	0.6931	0.6627	0.6471	0.6152
ΔG = - RTLnK_d (kJ/mol)	-1.7172	-1.6694	-1.6839	-1.6521

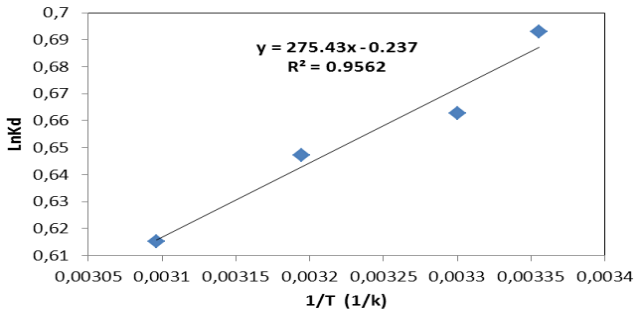

Fig. 14. The variations of LnK_d as a function of $\frac{1}{T}$

4. Conclusions

The present paper demonstrated that the activated carbon elaborated from *Juniperus thurifera* tree could be used as a low-cost and effective adsorbent for phenol removal. In the light of the above discussions, we can conclude that:

- The optimum pH should be between 3.4 whereas the optimum initial phenol concentration should be 50 mg/L.
- The obtained results show that adsorption kinetics follow the rate of pseudo-first-order ($R^2 = 0.9950$).
- The analysis of the equilibrium best fitted Freundlich ($R^2 = 0.9893$).
- The data obtained indicate that the absorption of phenol over activated carbon can be considered as physical adsorption.
- Thermodynamic findings proved that the absorption of phenol on activated carbon is spontaneous and exothermic.

References

[1] Damjanović, L.; Rakić, V.; Rac, V.; Stošić, D.; Auroux, A. The Investigation of Phenol Removal from Aqueous Solutions by Zeolites as Solid Adsorbents. *J. Hazard. Mater*. **2010**, *184*, 477-484. https://doi.org/10.1016/j.jhazmat.2010.08.059
[2] Lin, S.H.; Juang, R.S. Adsorption of Phenol and Its Derivatives from Water Using Synthetic Resins and Low-Cost Natural Adsorbents: A Review. *J. Environ. Manage*. **2009**, *90*, 1336-1349. https://doi.org/10.1016/j.jenvman.2008.09.003
[3] Megharaj, M.; Pearson, H.W.; Venkateswarlu, K. Toxicity of Phenol and Three Nitrophenols Towards Growth and Metabolic Activities of Nostoc Linckia, Isolated from Soil. *Arch. Environ. Contam. Toxicol*. **1991**, *21*, 578-584. https://doi.org/10.1007/BF01183881
[4] Yang, L.; Wang, Y.; Song, J.; Zhao, W.; He, X.; Chen, J.; Xiao, M. Promotion of Plant Growth and in situ Degradation of Phenol by an Engineered *Pseudomonas fluorescens* Strain in Different Contaminated Environments. *Soil Biol. Biochem*. **2011**, *43*, 915-922. https://doi.org/10.1016/j.soilbio.2011.01.001
[5] *World Health Organization, Guidelines for Drinking Water Quality, Health Criteria and Supporting Information*; World Health Organization: Geneva, Switzerland, 1984; pp. 1-127.
[6] Dutta, N.N.; Brothakur, S.; Baruah, R. A Novel Process for Recovery of Phenol from Alkaline Wastewater: Laboratory Study and Predesign Cost Estimate. *Water Environ. Res*. **1998**, *70*, 4-9. https://doi.org/10.2175/106143098X126838
[7] Baup, S.; Jaffre, C.; Wolbert, D.; Laplanche, A. Adsorption of Pesticides onto Granular Activated Carbon: Determination of Surface Diffusivities Using Simple Batch Experiments. *Adsorption* **2000**, *6*, 219-228. https://doi.org/10.1023/A:1008937210953
[8] Md Ahmaruzzaman. Adsorption of Phenolic Compounds on Low-Cost Adsorbents: A Review. *Adv. Colloid Interface Sci*. **2008**, *143*, 48-67. https://doi.org/10.1016/j.cis.2008.07.002
[9] Kim, T.Y.; Jin, H.J.; Park, S.S.; Kim, S.J.; Cho, S.Y. Adsorption Equilibrium of Copper Ion and Phenol by Powdered Activated Carbon, Alginate Bead and Alginate-Activated Carbon Bead. *J. Ind. Eng. Chem*. **2008**, *14*, 714-719. https://doi.org/10.1016/j.jiec.2008.07.004
[10] Fan, J.; Zhang, J.; Zhang, C.; Ren, L.; Shi, Q. Adsorption of 2,4,6-Trichlorophenol from Aqueous Solution onto Activated Carbon Derived from *loosestrife*. *Desalination* **2011**, *267*, 139-146. https://doi.org/10.1016/j.desal.2010.09.016
[11] Haghighat, M.H.; Mohammad-Khah, A. Removal of Trihalomethanes from Water using Modified Montmorillonite. *Acta Chim. Slov*. **2020**, *67*, 1072. http://dx.doi.org/10.17344/acsi.2020.5832
[12] Ren, S.; Deng, J.; Meng, Z.; Wang, T.; Xie, T.; Xu, S. Enhanced Removal of Phenol by Novel Magnetic Bentonite Composites Modified with Amphoteric-Cationic Surfactants. *Powder Technol*. **2019**, *356*, 284-294. https://doi.org/10.1016/j.powtec.2019.08.024
[13] Ouallal, H.; Dehmani, Y.; Moussout, H.; Messaoudi, L.; Azrour, M. Kinetic, Isotherm and Mechanism Investigations of the Removal of Phenols from Water by Raw and Calcined Clays. Heliyon **2019**, *5*, e01616. https://doi.org/10.1016/j.heliyon.2019.e01616
[14] Bouiahya, K.; Es-saidi, I.; El Bekkali, C.; Laghzizil, A.; Robert, D.; Nunzi, J.M.; Saoiabi, A. Synthesis and Properties of Alumina-Hydroxyapatite Composites from Natural Phosphate for Phenol Removal from Water. *Colloids Interface Sci. Commun*. **2019**, *31*, 100188. https://doi.org/10.1016/j.colcom.2019.100188
[15] Liao, Q.; Sun, J.; Gao, L. The Adsorption of Resorcinol from Water Using Multi-Walled Carbon Nanotubes. *Colloids Surf. A: Physicochem. Eng. Asp*. **2008**, *312*, 160-165. https://doi.org/10.1016/j.colsurfa.2007.06.045
[16] Chakraborty, A.; Deva, D.; Sharma, A.; Verma, N. Adsorbents Based on Carbon Microfibers and Carbon Nanofibers for the Removal of Phenol and Lead from Water. *J. Colloid Interface Sci*. **2011**, *359*, 228-239. http://dx.doi.org/10.1016/j.jcis.2011.03.057
[17] Sulaymon, A.H.; Ahmed, K.W. Competitive Adsorption of Furfural and Phenolic Compounds onto Activated Carbon in Fixed Bed Column. *Environ. Sci. Technol*. **2008**, *42*, 392-397. https://doi.org/10.1021/es070516j
[18] Okasha, A.Y.; Ibrahim, H.G. Phenol Removal from Aqueous Systems by Sorption of Using Some Local Waste Materials. *Elec. J. Env. Agricult. Food Chem*. **2010**, *9*, 796-807.
[19] Senthilkumaar, S.; Krishna, S.K.; Kalaamani, P.; Subburamaan, C.V.; Ganapathi Subramaniam, N. Adsorption of Organophosphorous Pesticide from Aqueous Solution Using "Waste" Jute Fiber Carbon. *Mod. Appl. Sci*. **2010**, *4*, 67-83.
[20] Ekop, A.S.; Eddy, N.O. Thermodynamic Study on the Adsorption of Pb^{2+} and Zn^{2+} From Aqueous Solution by Human Hair. *J. Chem*. **2010**, *7*, 849239. https://doi.org/10.1155/2010/849239
[21] Mukherjee, S.; Kumar, S.A.; Misra, K.; Fan, M. Removal of Phenols from Water Environment by Activated Carbon, Bagasse Ash and Wood Charcoal. *Chem. Eng. J*. **2007**, *129*, 133-142. https://doi.org/10.1016/j.cej.2006.10.030

[22] Gauquelin, T.; Bertaudière, V.; Cambecèdes, J.; Largier, G. Le Genevrier Thurifere (Juniperus Thurifera L.) Dans les Pyrenees: Etat de Conservation et Perspectives. *Acta Bot. Barc*. **2003**, *49*, 83-94.
[23] Humelnicu, D.; Ignat, M.; Suchea, M. Evaluation of Adsorption Capacity of Montmorillonite and Aluminium-pillared Clay for Pb^{2+}, Cu^{2+} and Zn^{2+}. *Acta Chim. Slov*. **2015**, *62*, 947. http://dx.doi.org/10.17344/acsi.2015.1825
[24] Maulina, S.; Mentari, V.A. IOP Conf. Series: Materials Science and Engineering, 2019; pp. 012023.
[25] Mahalakshmy, R.; Idraneel, P.; Viswanatan, B. Surface Functionalities of Nitric Acid Treated Carbon – A Density Functional Theory Based Vibrational Analysis. *Indian J. Chem*. **2009**, *48*, 352-356. http://nopr.niscpr.res.in/handle/123456789/3371
[26] El Nemr, A.; Abdelwahab, O.; El-Sikaily, A.; Khaled, A. Removal of Direct Blue-86 from Aqueous Solution by New Activated Carbon Developed from Orange Peel. *J. Hazard. Mater*. **2009**, *161*, 102-110. https://doi.org/10.1016/j.jhazmat.2008.03.060
[27] Yan, M.A.; Gao, N.; Chu, W.; Li, C. Removal of Phenol by Powdered Activated Carbon Adsorption. *Front. Environ. Sci. Eng*. **2013**, *7*, 158-165. https://doi.org/10.1007/s11783-012-0479-7
[28] Lagergren, S. Kungliga Svenska Vetenskapsakademiens. *Handlingar* **1898**, *24*, 1-39.
[29] Ho, Y.S.; McKay, G. Pseudo-Second Order Model for Sorption Processes. *Process. Biochem*. **1999**, *34*, 451-465. https://doi.org/10.1016/S0032-9592(98)00112-5
[30] Weber, W.J.; Morris, J.C. Advances in Water Pollution Research: Removal of Biologically Resistant Pollutant from Wastewater by Adsorption. In *Proceedings of 1st International Conference on Water Pollution Symposium*; Pergamon: Oxford, 1962; pp. 231-266.
[31] Hameed, B.H. Equilibrium and Kinetics Studies of 2,4,6-Trichlorophenol Adsorption onto Activated Clay. *Colloid Surf. A*: *Physicochem. Eng. Aspects* **2007**, *307*, 45-52. https://doi.org/10.1016/j.colsurfa.2007.05.002
[32] Langmuir, I. The Adsorption of Gases on Plane Surfaces of Glass, Mica and Platinum. *J. Am. Chem. Soc*. **1918**, *40*, 1361-1403. https://doi.org/10.1021/ja02242a004
[33] Ullah, H.; Nafees, M.; Iqbal, F.; Awan, S.; Shah, A.; Waseem, A. Adsorption Kinetics of Malachite Green and Methylene Blue from Aqueous Solutions Using Surfactant-Modified Organoclays. *Acta Chim. Slov*. **2017**, *64*, 449.
[34] Freundlich, H.M.F. Over the Adsorption in Solution. *J. Phys. Chem*. **1906**, *57*, 385-471.
[35] Senturk, I.; Alzein, M. Adsorption of Acid Violet 17 onto Acid-Activated Pistachio Shell: Isotherm, Kinetic and Thermodynamic Studies. *Acta Chim. Slov*. **2020**, *67*, 55-69. https://doi.org/10.17344/acsi.2019.5195
[36] Temkin, M.I.; Pyzhev, V. Kinetics of Ammonia Synthesis on Promoted Iron Catalysts. *Acta Physicochim*. **1940**, *12*, 327-356.

Received: August 27, 2021 / Revised: September 07, 2021 / Accepted: October 30, 2021

ВИЛУЧЕННЯ ФЕНОЛУ З ВОДИ ЗА ДОПОМОГОЮ АКТИВОВАНОГО ВУГІЛЛЯ, ОТРИМАНОГО З ДЕРЕВА *JUNIPERUS TURIFERA*

Анотація. *Метою цієї роботи є дослідження доцільності використання активованого вугілля, отриманого з дерева Juniperus thurifera, як адсорбента для вилучення фенолу з води за допомогою адсорбції. Досліджено вплив початкової концентрації фенолу, часу контакту, pH і маси адсорбента на адсорбційну здатність фенолу. Найбільша адсорбційна здатність досягається за pH=3,4, концентрації фенолу 50 мг/л, маси адсорбенту 100 мг і тривалості 24 год. Рівняння ізотерм Фрейндліха, Ленгмюра та Темкіна були використані для опису наших експериментальних даних. Встановлено, що модель Фрейндліха є найкращою моделлю з* $R^2 = 0{,}9893$*. Термодинамічні результати показали, що адсорбція фенолу на активованому вугіллі була спонтанною й екзотермічною. Крім того, дослідження кінетики адсорбції показало, що процес адсорбції відповідає кінетичній моделі псевдопершого порядку.*

Ключові слова: *активоване вугілля, дерева Juniperus thurifera, фенол, адсорбція.*